

Experimental analysis of the performances of ventilated photovoltaic facades

R. Arena¹, S. Aneli¹, G.M. Tina¹ and A. Gagliano¹

¹ Department of Electrical Electronic and Computer Engineering
University of Catania
Viale Andrea Doria,6, Catania (Italy)

Phone/Fax number:+0039 7382451, e-mail: roberta.arena@phd.unict.it, stefano.aneli@unict.it,
giuseppe.tina@unict.it, antonio.gagliano@unict.it

Abstract.

To reach the EU 2030 goals for reducing greenhouse gas emissions targets and achieving high-performing buildings, it is mandatory to increase energy generation through renewable sources. In this context, existing and new buildings should be equipped with building-integrated photovoltaic plants (BiPV). However, BiPV system integration into the building envelope could harm the electrical efficiency due to an increase in the temperature of the cells.

The purpose of this work is to analyse the performance of BiPV façade naturally ventilated. With this aim, two prototypes of ventilated façade equipped with mono and bifacial PV modules have been realised. The first stage of this research presents the features of these two prototypes, the monitoring system and some preliminary experimental data. In particular, the daily temperatures of the flowing air in the cavity, on the front and the back of mono e bifacial modules are shown, during the investigated days. The observation allowed us to highlight the positive effects of the ventilated air gap, as well as the different behaviour of the two investigated PV facades. Further stages foresee the analysis of these BiPV ventilated facades through fluid dynamics simulations, as well as their electrical performance.

Key words. Ventilated façade, bifacial photovoltaic module,

Nomenclature

A apparent solar irradiation	[W/m ²]
AM air mass	[-]
B atmospheric extinction coefficient	[-]
β solar altitude above the horizontal	[°]
Y ratio between sky diffuse radiation on a vertical surface to that on a horizontal surface	[-]
Ed _n normal direct irradiation	[W/m ²]
Ed diffuse irradiation	[W/m ²]

1. Introduction

From the Industrial Revolution to today, energy consumption continues to grow from year to year; initially, the most used resource was coal, while oil from 1900 has dominated the market. Nevertheless, fossil sources cause various environmental problems, the most important being

the emission of greenhouse gases, for example, CO₂, which contribute to global warming. The content of carbon dioxide in the atmosphere, as recorded and reported by the Mauna Loa Observatory in Hawaii, continuously grow from 1960, and the slope of the curve is increasing [1]. One of the most impactful sectors is construction, as reported by the IEA (International Energy Agency). The buildings and buildings construction sectors are responsible for over one-third of global final energy consumption and nearly 40% of total direct and indirect CO₂ emissions, 9 Gt in 2020 [2]. Therefore, a breakthrough is mandatory, shift to renewable energy sources, which have low environmental effects and are not subject to depletion is mandatory. Nearly Zero Energy Building (NZEB) can be one of the solutions to this problem. In fact, NZEB has very high-energy performances [3] [4]; and the very low or almost zero energy demand should be satisfied through renewable sources [5].

One of the techniques that can be used in buildings to reduce energy consumption concerns the construction of ventilated roofs and façades, whose external cladding system creates an air gap with the perimeter envelope of the building [6]. In the summer period, the increase of the air temperature in the cavity due to solar radiation that hits the external surface causes the so-called "chimney effect", which in turn generates the upward motion of air [7]. In this way, the outdoor flowing air cools the facade reducing the temperature on the inner wall. In the winter months, however, when the radiation is less intense, the cavity keeps the internal temperature of the wall in equilibrium, thus reducing the problems related to the risk of surface condensation [8].

In addition, ventilated façades can also be a support for the installation of photovoltaic modules, thus creating a BiPV system (Building Integrated Photovoltaic), as well as photovoltaic thermal panes (PVT) [9]. The performance of photovoltaic modules is sensitive to temperature; it decreases by 5% every 10 °C of the temperature increase, so the adoption of cooling techniques, active or passive is recommended [10].

Passive cooling techniques can include Phase Change Materials (PCM). This substance as reported in the study of Aneli et al. allows to obtain an increase of 3.5% of the energy produced in a year, but the type of PCM to be used must be carefully chosen, evaluating the time assuring its complete melting/solidification [11].

The "chimney effect" in the ventilated PV façade allows the cooling of the modules installed, so increasing considerably the PV cell efficiency in the hottest periods [12].

Ritzen et al. explored the effects of ventilation on a BIPV system installed on the roof of a building and found that ventilation is an effective method to prevent modules from accumulating too much heat causing decreased performance and possible technical problems [13].

Yang et al. have studied the application of BIPV systems on facades in three different cities of Australia with three different modes of operation: non-ventilated, naturally ventilated and mechanically ventilated. From the analysis carried out, it appears that the best mode of operation varies according to the climate conditions. In general, it seems that in warmer climates, it is preferable to ventilate mechanically the façade, but in colder ones, a distinction is necessary. In fact, if the goal is to reduce the thermal loads then the best operation mode is the non-ventilated one, but in terms of energy savings, the best mode of operation is the naturally ventilated [14].

The work reported is the latest in a series of studies that have highlighted several important aspects of this technology.

Gagliano et al. studied the performance of a ventilated façade during the winter and summer, as a function of the façade exposure and wind speeds. They found the ventilated façade had temperatures even 20 °C lower than a non-ventilated façade in both seasons. The amount of savings varies greatly in the winter season depending on exposure and wind; in fact, it fluctuates between 20% for facades exposed to the East/ West and 50% for facades facing south. Instead, the savings obtained in the summer are more constant and vary between 40 and 50% [15].

Tina et al. compared the thermal behaviour of three facades, two of them made with monofacial PV modules and just one of them ventilated, as the third one is composed of bifacial PV modules. It was noticed that the active ventilation has decreased temperatures by even 5°C; furthermore, being semi-transparent, the bifacial PV module recorded temperature 1-2°C lower than the PV one. Finally, simulations carried out with PVsyst showed the effect of ventilation on the performance of mono and bifacial facades compared to the monofacial non-ventilated one, obtaining higher values respectively of the 5% and 13.5% [16]. However, in the current literature, there are not many studies that evaluate the performances of photovoltaic ventilated façades realised with bifacial PV modules.

This paper presents a study on the thermal behaviour of two photovoltaic ventilated façades, realized with mono and bifacial PV modules respectively. The work carried out consists of two main phases: the first, which is discussed in this article, provides for the collection and analysis of the experimental data obtained from the monitoring of the ventilated PV facades. The second part of this study, which is currently under progress, is focused on the development of a fluid dynamic numerical model of the PV facades through the software Ansys Fluent [17].

2. Material and Methods

The analysis of the thermal behaviour of a ventilated facade is a very complex task. Indeed, it has to be considered the interactions between the airflow within the ventilated gap of the facade and the forcing environmental variables. Such interactions are driven by the heat fluxes between the facade and the environments determined by conduction, convection and thermal radiation.

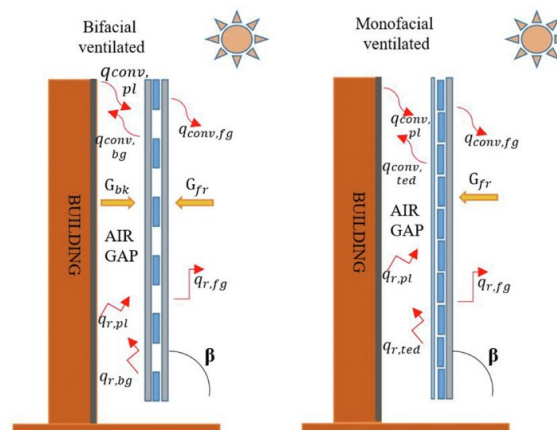


Figure 1: Heat Fluxes between the PV facade, bifacial (left) and monofacial (right) modules, to the outdoor environment

Figure 1 shows the heat fluxes acting on the two PV facades, that are:

- conduction between multilayer elements
- convection/radiation between the external surface of the system and the surrounding environment ($q_{conv,fg}/q_{r,fg}$)
- convection due to the air flow on the two sides of the ventilated cavity ($q_{conv,bg}/q_{conv,pl}$)
- solar radiation on the outermost surface of the model (G_{fr})
- radiative exchange between the two sides of the ventilated cavity ($q_{r,bg}/q_{r,pl}$)

The second part of this study, which is currently under progress, is focused on the development of a fluid dynamic numerical model of the PV facades through the software Ansys Fluent.

The investigated ventilated facades are represented by a 3D geometry in order to evaluate in the more realistic way the heat fluxes as well the fluid-dynamic within the air gap. Another central plus of 3D model, it is the possibility of giving as input the hourly solar irradiance that hits a surface of all year around by using the Fluent's solar calculator. To achieve this the day, the time, the mesh orientation, as well as information related to the global position, namely, latitude, longitude and time zone of the location have to be provided [18].

In this way, the solar radiation is computed as a heat source and it is implemented in the energy equations.

Furthermore, it is possible to select the calculation option between "Fair Weather Conditions and Theoretical Maximum Method". In the first case, the solar radiation is

attenuated considering meteorological conditions closer to the real ones. The equation for normal direct irradiation is determined from the ASHRAE Handbook [19].

$$E_{dn} = \frac{A}{\frac{B}{e^{\sin(\beta)}}} \quad (1)$$

The diffuse irradiation is calculated from the normal direct irradiation through the following formula, for vertical surfaces:

$$E_d = CYE_{dn} \quad (2)$$

where:

- A is the apparent solar irradiation at air mass AM=0,
- B the atmospheric extinction coefficient for a clear day,
- β is the solar altitude (in degrees).
- C is a constant and
- Y is the ratio between sky diffuse radiation on a vertical surface to that on a horizontal surface [19].

The radiative fluxes are calculated using the Discrete Ordinates (DO) model, which solves the radiative transfer equation (RTE) for a finite number of discrete solid angles [20].

3. Description of the experimental PV facade

The two vertical ventilated photovoltaic facades analysed in this study, with tilt and azimuth angle of 90 and 19° respectively, are positioned on the roof of the DIEEI, at the University of Catania (Latitude 37.52 North, Longitude 15.07 East).

The first facade is realised with two mono facials (glass-temlar), while the other with two bifacial (glass-glass) photovoltaic modules (bPV). The PV modules are distanced from the building wall, so a ventilated air gap, thickness of 14 cm, is created, the outdoor air come in from an opening of 25 cm at the bottom and goes out from an opening of 10 cm at the top of the air gap. The backside of the glass bPV module, which is semi-transparent, is hit by the solar irradiation reflected from the building wall placed behind the BIPV facades.

The remaining part of the front of the ventilated facade, not filled with the PV panels, is made with opaque fiber cement panels. Only a strip of structure between the two bifacial modules is realised with a semi-transparent material. On this strip, a pyranometer for detecting the irradiation reflected by the building wall is placed. In this way, the irradiance that strikes the backside of the bifacial modules is measured. The monofacial and bifacial modules are both made of monocrystalline silicon. The bifacial bPV module applies the Hetero Junction Technology (HJT) that guarantees high performance and low degradation.

The specifications of the two PV modules, mono and bifacial, are given in Table 1.

Peak Power	245 W	340 W
STC Efficiency	13%	17%
Temperature Coefficient	-0.44%/°C	-0.38%/°C
Bifaciality Factor	/	> 85%

The ventilated BIPV facades are continuously monitored with a weather station connected to a data logger that records the data detected every minute by the sensors installed, listed in table 2.



Figure 2: The Ventilated Facade

Figure 3 shows the positions of the above-mentioned sensors.

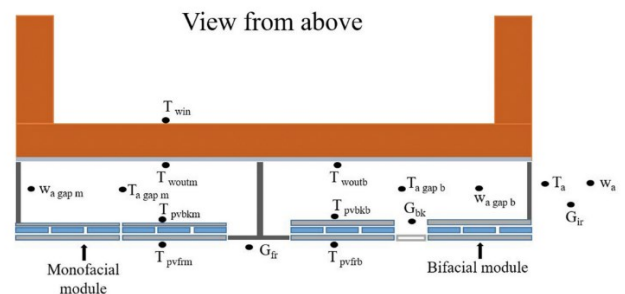


Figure 3: Position of the Sensors

The weather data are measured by: three pyranometers for the measurement of the horizontal, vertical and diffuse global irradiance, a rotary band heliometer for direct normal irradiance, the tacogonium anemometer for wind speed and direction. The temperature and humidity sensors are positioned within a radiant screen to exclude the influence of radiation. The pyranometer used for the diffuse component has an opaque band for shading the direct component of the solar irradiation. Moreover, a pyranometer, operating with a reference cells, detects the irradiance reflected by the building wall behind the PV facade (G_{fr}). The air temperature sensors detect: the temperatures of the air flow in the two air gaps ($T_{a,gap,m}$; $T_{a,gap,v}$), the temperature on the front ($T_{pv,fr,m}$; $T_{pv,fr,b}$) and back ($T_{pv,bk,m}$; $T_{pv,bk,b}$) of the PV module and on the wall behind ($T_{w,out}$, T_{win}) the PV facade.

Table 1: Electrical Characteristics of the Modules

	Monofacial	Bifacial
--	------------	----------

4. CFD modelling

The geometry of the facade has been simulated considering the stratigraphy reported in table 3.

Building the mesh is a very important step in the realization of a fluid dynamic simulation, and great accuracy is necessary to find the most suitable one. In fact, it is important to take into account that the characteristics of the mesh affect the accuracy, convergence and speed of the simulation. For instance, the denser the mesh, the more accurate the solution will be, but at the same time, the presence of a greater number of cells will increase the computation time. The various elements of the mesh, in fact, determine the volumes and the points in which the governing equations will be solved. Another important aspect concerns the type of elements the mesh is made of, they can be 1D, 2D, or 3D with varying aspect ratios. The fundamental element types used for constructing meshes are quadrangular or triangular for 2D geometries and hexahedral or tetrahedral for 3D ones. In our case, we employed tetrahedral elements.

Two different meshes have been realised. The first has larger dimensions, which allows reducing the calculation time, the second mesh has thicker dimensions as well as the geometry of the facade has been defined with more details to assess the reliability of the results.

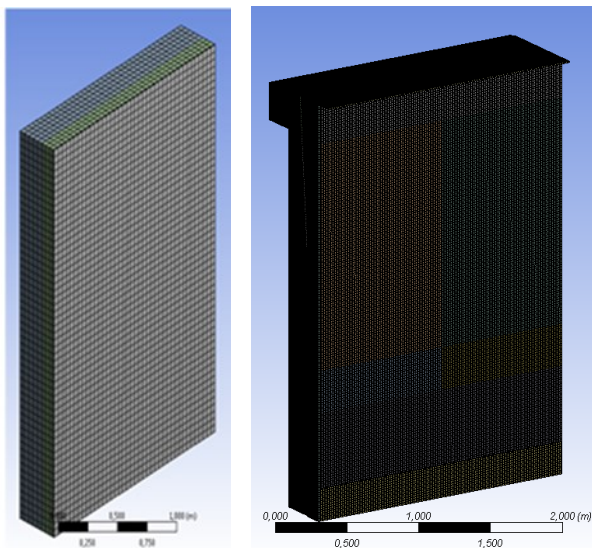


Figure 4: Mesh Realized

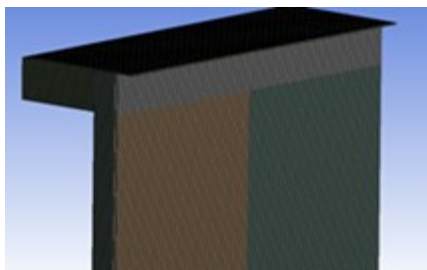


Figure 5: Detail of the Dense Mesh

The first mesh generated was made of 20,000 quadrangular elements, the largest have dimensions of $0.99 \cdot 10^{-2}$ m and the smallest $0.36 \cdot 10^{-2}$ m. Its quality has been checked with orthogonal quality and standard deviation parameters, which are respectively 0.99 and 0.2. The densest mesh is formed by 2,597,540 quadrangular elements whose dimensions vary between $0.89 \cdot 10^{-3}$ m and $1.0 \cdot 10^{-3}$ m,

and they present an orthogonal quality of 0.99 and standard deviation equal to $8 \cdot 10^{-3}$. Figure 4 shows a details of the computational domain and the mesh of calculus for the larger (left) and the densest mesh (right).

5. Results of the monitoring

This section illustrates some of the results derived from the monitoring of the photovoltaic ventilated facade. Figure 5 shows the irradiance values measured on February 24, In particular, the direct, diffuse, horizontal and vertical global irradiance are depicted. In addition, the irradiance reflected from the rear building wall is reported. This irradiation allows evaluating the contribution of the rear cells of the bifacial PV module on the power production. The electrical performances of the investigated facade will be presented in further studies.

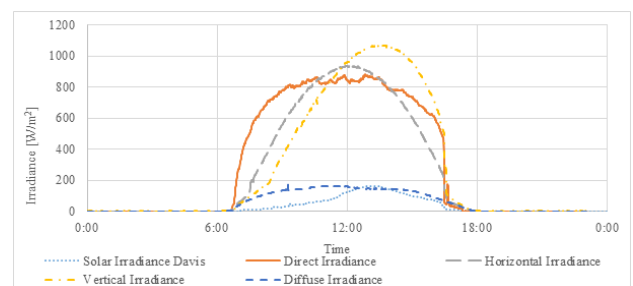


Figure 6: measured components of the solar radiation: global GHI (grey), GVI (yellow), E_{dn} (orange), E_d (blue), rGVI (point-dashed sky blue).

All the measured components of the solar radiation, i.e. global horizontal (GHI) and vertical (GVI), direct normal (E_{dn}) and diffuse (E_d) indicate that almost clear sky condition characterizes the investigated day. Considering that the facade faces South-West the peak of the irradiance on the facade is not recorded at noon, but between 14:30 and 15:00 in accordance with its orientation.

The reflected irradiance measured by the Davis sensors (rGVI) allows quantifying the amount of the solar irradiance that hits the rear face of the bPV module. It is possible to observe that it reaches a maximum of 160 W/m^2 , with total energy about 0.76 kWh/m^2 . Thus, considering an efficiency of the PV cell equal to 15% an extra energy yield of about 0.11 kWh/m^2 per day is obtained respect to a mono facial PV module.

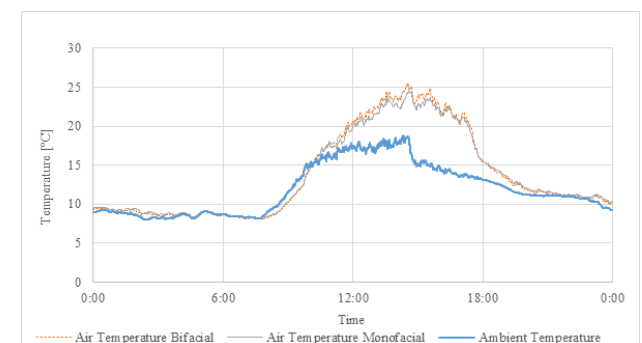


Figure 7: measured air temperatures at the exit of the cavity behind the mono (grey) and bifacial (orange) PV facades, as well as the outdoor ambient air temperature (blue).

Figure 7 shows the temperature measured at the exit of the cavity behind the mono (grey) and bifacial (orange) PV

façades, as well as the outdoor ambient air temperature (blue).

It is evident a marked difference between the ambient temperature and the temperature in the cavity, of around 7-8 °C, especially in the middle hours of the day, while in the night hours this difference tends to disappear. This means that during the daily hours the thermal dispersions from the indoor environment are significantly reduced. The air temperatures behind the bPV façade are slightly higher than the air temperatures behind the mono facial PV façade. This is due to the transparency of the bifacial module that allows the passage of a portion of the solar radiation that hits the rear-building wall. Therefore, it increases its temperature and in turn, the air flowing within the cavity is heated.

Figure 8 shows the daily variations of the temperatures measured on the front and back surface of the PV modules and on the wall behind the PV façades.

Unfortunately, we cannot show the temperature on the front of the bPV module due to the malfunctioning of this sensor.

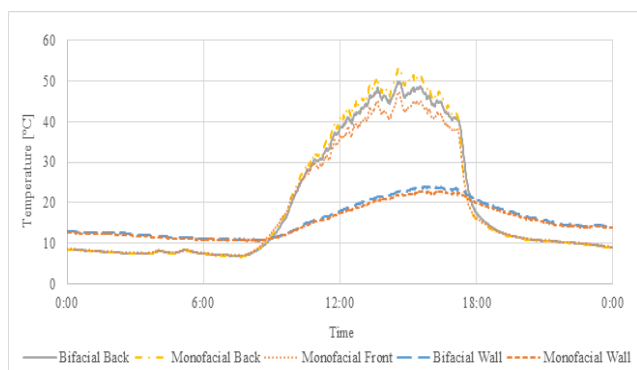


Figure 8: superficial temperatures measured: on the back of the bPV (grey), on the back (yellow) and front (orange) of the monofacial mPV, on the wall behind the bPV (blue sky) and mPV module (dark orange).

During the daily hours, the temperatures recorded on the backside of the bPV module are higher than the analogous temperatures of the mPV module. The same behaviour is observed for the surface temperatures on the wall behind the PV façades. Once again, this effect is determined by the passage of solar irradiance through the semi-transparent surface of the bPV module.

For the mPV module, the front temperature is lower than the temperatures recorded on the back. This effect is determined by the cooling action of the wind on the surface, reported in figure 9. As previously mentioned, we cannot provide such comparison for the bPV module due to the lack of data for the front temperature.

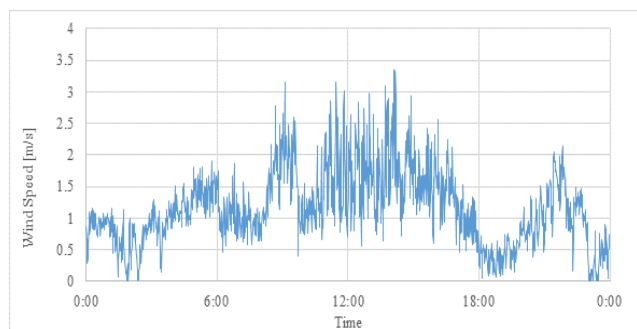


Figure 9: measured wind velocity.

During the night all the measured temperatures on the PV module (back and front) as well as on the wall behind the façades tends to be similar.

4. Conclusion

This study, focused on the thermal behaviour of BIPV ventilated façade, shows the results obtained from the monitoring system installed.

The temperatures observed on the PV modules, the air within the air gap, and on the rear-building wall are reported. It is interesting to notice the high impact of the ventilation on the temperature of the PV modules, and on the rear-building wall, due to the enhanced heat transfer. Consequently, an increase of the PV modules efficiency and the decrease of building thermal load is achieved. Moreover, the different behaviours between mono and bifacial module are highlighted.

The advantages achievable by this technology can be several: to cool down the temperature of photovoltaic modules and consequently increase the electrical production, reduce the temperature gradient on the building envelope, so reducing both thermal losses and solar gains. In fact, during the summer, the building envelope is shielded by the solar radiation and the air flow inside the cavity, triggered by the chimney effect, promotes the expulsion of the hottest air from the top of the façade. During the winter months, the air flow in the cavity tends to remain quiet. Thereby, the thermal dispersions from the heated rooms to the outside and the risks of mold and condensation are reduced.

Furthermore, the PV façade contributes to improving the acoustic performance and protecting the exterior envelope against atmospheric agents and pollutants widespread in our cities.

The main disadvantages of these systems are the cost and space required for the construction of the structure, the increased vulnerability to the fire of the building due to the chimney effect. However, the latest can be controlled with correct sizing of the cavity and using fireproof and self-extinguishing materials.

Further development of this study will be devoted to present the fluid dynamic simulation, as well as to present the electrical performance of these two PV ventilated façades.

Table 2: Type and characteristics of the installed sensors

	Pyranometer	Rotary Band Helimeter	Tacogoniometer	Air Temperature Sensor	Humidity and Air Temperature	Surface Temperature	Pyranometer
							
Measuring Range	0-4000W/m ²	0-1500W/m ²	0-75 m/s	-50 +70°C	-50 +100°C	-50 +70°C	0-1800 W/m ²
Accuracy	5%	15%	1% direction 2-3% velocity	0.15 °C	0.1 °C temp 1% hum.	0.1	5%
Response Time	20 s		0.9 s	30 s	10 s	30 s	

Table 3: Stratigraphy of the ventilated facade

Layer	Material	Thickness [cm]	Density [kg/m ³]	Thermal Conductivity [W/mK]	Specific Heat [J/kg K]	Type
Rear Wall	Brick Wall	25	2500	0.9	1000	Solid
Air Chamber	Air	14	1.225	0.0242	1006.43	fluid
Front Wall	Solar Module	1	2300	1	960	solid
	Aqua Panel	1	1200	0.4	1000	solid

Acknowledgement

This research is funded by the " research project PIACERI 2020" of the Department of Electric, Electronics and Computer Engineering of the University of Catania.

References

- [1] NOAA Research News <https://research.noaa.gov/article/ArtMID/587/ArticleID/2764/Coronavirus-response-barely-slows-rising-carbon-dioxide>.
- [2] Buildings: A source of enormous untapped efficiency potential <https://www.iea.org/topics/buildings>.
- [3] M. Cellura, F. Guarino, S. Longo, M. Mistretta, "Energy life-cycle approach in Net zero energy buildings balance: Operation and embodied energy of an Italian case study", *Energy and Buildings* (2014). Vol. 72 pp. 371-381.
- [4] H. Erhorn, H. Erhorn-Kluttig: 'Towards 2020 – Nearly zero-energy buildings', published in book: *Implementing the Energy Performance of Buildings Directive (EPBD) – Featuring Country Reports, 2015. Report of the EU Concerted Action EPBD project, December 2015*, www.epbd-ca.eu.
- [5] A Monteleone, G Rodonò, A Gagliano, V Sapienza SLICE: An Innovative Photovoltaic Solution for Adaptive Envelope Prototyping and Testing in a Relevant Environment, *Sustainability*
- [6] V. Bianco, A. Diana, O. Manca, S. Nardini, "Numerical investigation of an inclined rectangular cavity for ventilated roofs applications, *Thermal Science and Engineering*, (2018)
- [7] H Elarga, S Fantucci, V Serra, R Zecchin, E Benini Experimental and numerical analyses on thermal performance of different typologies of PCMs integrated in the roof space- *Energy and buildings*, (2017)..
- [8] D. Li, Y. Zheng, C. Liu, H. Qi, X. Liu, "Numerical analysis on thermal performance of naturally ventilated roofs with different influencing parameters", *Sustainable Cities and Society* (2016), Vol. 22, pp. 86-93.
- [9] A Gagliano, GM Tina, S Aneli, D Chemisana, Analysis of the performances of a building-integrated PV/Thermal system
- [10] P. Bevilacqua, A. Morabito, R. Bruno, V. Ferraro, N. Arcuri, "Seasonal performances of photovoltaic cooling systems in different weather conditions", *Journal of Cleaner Production* (2020), Vol. 272.
- [11] S. Aneli, R. Arena, A. Gagliano, "Numerical Simulations of a PV Module with Phase Change Material (PV-PCM) under Variable Weather Conditions", *International Journal of Heat and Technology* (2021), Vol. 39 pp. 643-652.
- [12] GM Tina, FB Scavo, A Gagliano Multilayer thermal model for evaluating the performances of monofacial and bifacial photovoltaic modules *IEEE Journal of Photovoltaics* 10 (4), 1035-1043
- [13] M.J. Ritzen, Z.A.E.P. Vroon, R. Rovers, C.P.W. Geurts, "Comparative performance assessment of a non-ventilated and ventilated BIPV rooftop configurations in the Netherlands", *Solar Journal* (2017), Vol. 146, pp. 389-400.
- [14] S. Yang, A. Cannavale, A. Di Carlo, D. Prasadd, A. Sproul, F. Fiorito, "Performance assessment of BIPV/T double-skin façade for various climate zones in Australia: Effects on energy consumption", *Solar Energy* (2020), Vol. 199, pp. 377-399.
- [15] A Gagliano, S Aneli, "Analysis of the energy performance of an Opaque Ventilated Façade under winter and summer weather conditions", *Solar Energy* (2020), pp. 531-544.
- [16] G.M. Tina, F.B. Scavo, S. Aneli, A. Gagliano, "Assessment of the electrical and thermal performances of building integrated bifacial photovoltaic modules", *Journal of Cleaner Production* (2021), Vol. 313.
- [17] Ansys <https://www.ansys.com/it-it/products/fluids/ansys-fluent#tab1-1>
- [18] <https://www.afs.enea.it/project/neptunius/docs/fluent/html/ug/node1026.htm>
- [19] ASHRAE Handbook, Fundamentals Volume (5) 1985
- [20] P.Filipović, D. Dović, B. Ranilović, I. Horvat Numerical and experimental approach for evaluation of thermal performances of a polymer solar collector, *Renewable and Sustainable Energy Reviews*, Vol 112, September 2019, Pages 127-139